

Sensory and Motor Systems

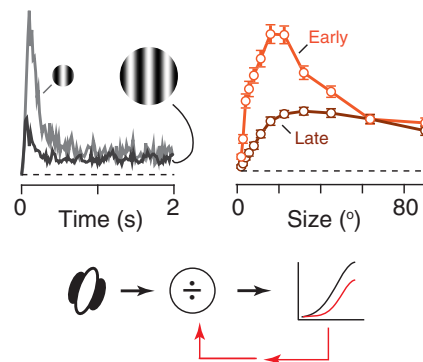
Dynamic Contextual Modulation in Superior Colliculus of Awake Mouse

Gioia De Franceschi and Samuel G. Solomon

<https://doi.org/10.1523/ENEURO.0131-20.2020>

Institute of Behavioural Neuroscience, Department of Experimental Psychology, University College London, London WC1H 0AP, United Kingdom

Visual Abstract



The responses of neurons in the visual pathway depend on the context in which a stimulus is presented. Responses to predictable stimuli are usually suppressed, highlighting responses to unexpected stimuli that might be important for behavior. Here, we established how context modulates the response of neurons in the superior colliculus (SC), a region important in orienting toward or away from visual stimuli. We made extracellular recordings from single units in the superficial layers of SC in awake mice. We found strong suppression of visual response by spatial context (surround suppression) and temporal context (adaptation). Neurons showing stronger surround suppression also showed stronger adaptation effects. In neurons where it was present, surround suppression was dynamic and was reduced by adaptation. Adaptation's effects further revealed two components to surround suppression: one component that was weakly tuned for orientation and adaptable, and another component that was more strongly tuned but less adaptable. The selectivity of the tuned component was flexible, such that suppression was stronger when the stimulus over the surround matched that over the receptive field. Our results therefore reveal strong interactions between spatial and

Significance Statement

Our senses provide enormous amounts of information, and the central nervous system needs to filter this information to focus on potentially important objects. Here, we study two visual mechanisms that might highlight unexpected or surprising objects for further analysis: surround suppression and adaptation. We show that both mechanisms work to filter the neural signals provided by the superior colliculus (SC), a midbrain area important for directing behavior. We also show that the two mechanisms are unexpectedly intertwined, endowing rich dynamics on neural signals at the first central stage of sensory processing. Finally, our results suggest a subpopulation of neurons that is specialized for signaling the presence of potentially important objects.

temporal context in regulating the flow of signals through mouse SC, and suggest the presence of a subpopulation of neurons that might signal novelty in either space or time.

Key words: adaptation; functional properties; non-classical receptive field; suppression; tectum; vision

Introduction

Unexpected objects are likely to be important for behavior, and predictable objects less important. Many aspects of the functional organization of the visual system can be explained by supposing that neuronal activity is suppressed when the image falling on a receptive field is predictable. For example, inhibitory inputs to retinal neurons can be thought of as providing predictions about the intensity of the image over the receptive field, suppressing responses unless the intensity deviates from those predictions (Srinivasan et al., 1982). The functional consequences of this predictive inhibition are the classical center-surround organization and transient responses of receptive fields in the retina and its targets (Hartline, 1940; Kuffler, 1953; Barlow, 2001).

In the classical model of an early receptive field, inhibition provides predictions about the average intensity of the image over the receptive field, but not the variance, or pattern, of intensity in that image. Two additional mechanisms are needed to explain how responses to predictable patterns are suppressed. Spatial interactions (often called surround suppression) can suppress responses when the pattern over the classical receptive field (CRF) is similar to that in the surrounding region. Temporal interactions (often called adaptation) can suppress responses when the pattern is similar over time. The spatial and temporal suppression are thought to reflect the action of “gain controls,” mechanisms that regulate the responses generated by the CRF (Shapley and Victor, 1978; Bonds, 1989; Carandini and Heeger, 2011; Solomon and Kohn, 2014; Webster, 2015).

While most work on spatial and temporal gain controls has concentrated on visual cortex (Allman et al., 1985; Solomon and Kohn, 2014; rodent: Adesnik et al., 2012; Vaiceliunaite et al., 2013; Self et al., 2014; cat: Movshon and Lennie, 1979; Carandini and Ferster, 1997; monkey: Mayo and Sommer,

2008; Patterson et al., 2013), gain controls are also known to be important in the retina and early stages of central visual processing (rodent: Zhang et al., 2012; Jacoby and Schwartz, 2017; lagomorphs: Oyster and Takahashi, 1975; Smirnakis et al., 1997; cat: Sterling and Wickelgren, 1969; Jones et al., 2000; Bonin et al., 2005; Fisher et al., 2017; monkey: Solomon et al., 2002, 2004, 2006; Boehnke et al., 2011). In most animals the major target of the retina is the superficial layers of the midbrain superior colliculus (SC; homologous to the optic tectum; May, 2006; Ellis et al., 2016). The superficial layers of SC (SCs) project to, among other areas, the deeper layers of SC, which are important in organizing movements toward or away from potentially important objects (Dean et al., 1989; Basso and May, 2017; rodent: Comoli et al., 2012; Hoy et al., 2019). The receptive fields of superficial SC neurons are often remarkably selective for image features: for example, neurons in superficial SC of mouse can be tightly tuned for contour orientation, even in the absence of visual cortex (Wang et al., 2010; Shi et al., 2017). The receptive fields of neurons in superficial SC also show prominent surround suppression (rodent: Girman and Lund, 2007; Wang et al., 2010; Ahmadiou et al., 2017; Barchini et al., 2018; monkey: Davidson and Bender, 1991) and adaptation (Dutta and Gutfreund, 2014; monkey: Boehnke et al., 2011). How gain controls influence the response of SC neurons is less clear, particularly in awake animals. For example, we do not know whether surround suppression and adaptation's effects are ubiquitous, whether they are independent, or how they interact.

Here, we made extracellular recordings from the superficial layers of SC in awake mice. We characterized surround suppression from the response to drifting gratings of varying size, and characterized adaptation from the time course of the response to drifting gratings of optimal size. We find profound impact of surround suppression and adaptation in many but not all neurons, and show that neurons with strong suppressive surrounds are also more susceptible to adaptation. Further, the suppressive surrounds themselves are susceptible to adaptation, and adaptation's effects reveal at least two components of suppression, an untuned component that is adaptable, and a tuned component that is less adaptable. The selectivity of the tuned component was not static, but flexible: that is, suppression depended on what was shown to the receptive field, and was stronger when the stimulus over the surround matched that over the receptive field. The spatial and temporal gain controls may therefore allow neurons in the superficial SC the capacity to dynamically signal unexpected events in either space or time.

Materials and Methods

Ethical approval

All animal procedures were performed in accordance with the United Kingdom Animals Scientific Procedures

Received April 4, 2020; accepted July 17, 2020; First published August 31, 2020.

The authors declare no competing financial interests.

Author contributions: G.D.F. and S.G.S. designed research; G.D.F. performed research; G.D.F. and S.G.S. analyzed data; G.D.F. and S.G.S. wrote the paper.

S.G.S. was supported by the Biotechnology and Biological Sciences Research Council Project Grant BB/R004765/1 and by an International Collaboration Award (with Adam Kohn) from the Stavros Niarchos Foundation/Research to Prevent Blindness. G.D.F. was also supported by an Impact studentship from University College London.

Acknowledgements: We thank A. Perry and N. Dhruv for help in early experiments.

Correspondence should be addressed to Gioia De Franceschi at gioia.defranceschi@embl.it.

<https://doi.org/10.1523/ENEURO.0131-20.2020>

Copyright © 2020 De Franceschi and Solomon

This is an open-access article distributed under the terms of the Creative Commons Attribution 4.0 International license, which permits unrestricted use, distribution and reproduction in any medium provided that the original work is properly attributed.

Act (1986). Experiments were performed at University College London in accordance with its animal care committee's regulations, under personal and project licenses released by the Home Office following appropriate ethics review, and in accordance with the ethical policy under which *eNeuro* operates.

General

Adult C57BL/6 male mice (8–12 weeks at the start of experiments, 20–35 g) were obtained from Charles River Laboratories. Animals were housed with *ad libitum* food and water, on an inverted 12/12 h light/dark cycle. Measurements were obtained during the dark phase. To prevent damage to implanted devices, animals were singly housed after the preparatory surgeries described below.

Preparation for recordings

Anesthesia was induced with 3% isoflurane in O₂ and the animal transferred to a stereotaxic apparatus. Anesthesia was subsequently maintained with 1–1.5% isoflurane in O₂, and adjusted as necessary by monitoring the breathing rate and absence of reflex responses to paw pinch. The scalp was retracted and a craniotomy was made in one hemisphere, centered 3.5–3.7 mm posterior to bregma, 0.7–1.1 mm lateral to the midline suture. A metal head postfixed to the skull and a ground screw implanted over frontal cortex. In six animals the brain was covered with a layer of Kwik-Cast Sealant (WPI), which was replaced with artificial cerebrospinal fluid (Bio-Techne Ltd) during recording sessions; in these cases, recordings were subsequently made using quartz/platinum-tungsten electrodes (Thomas Recordings; impedance 4–5 M Ω) or tetrodes (impedance 0.5–0.8 M Ω). In two animals the dura mater was instead removed and a 16-channel microdrive (arranged as four tetrodes; Axona Ltd) was implanted. Animals recovered from surgery for at least one week and were then habituated to head-restraint before recordings started. Typical duration of a recording session was 90–120 min. At the end of the experiments, animals were euthanized by overdose of sodium pentobarbital intraperitoneal.

Recordings and spike sorting

The analog signal from each electrode was amplified and filtered (0.3 kHz –7/10 kHz), then digitized and recorded at 48 or 44 kHz. All recordings obtained at one site on 1 d were analyzed together. Putative single units were identified off-line using Plexon Offline Sorter (version 3.3.2, for single electrode recordings) or KlustaSuite (Rossant et al., 2016). Single units were identified by clustering in principal component (PCA) space, followed by manual inspection of spike shape, auto-correlograms and cross-correlograms. In no putative single unit did the fraction of interspike interval (ISIs) under 0.5 ms exceed 2%.

Visual stimuli

Visual stimuli were generated using Expo (P. Lennie) on an Apple Macintosh computer, and presented on a LCD monitor (Iiyama ProLite E1890SD, mean luminance 35–45 candela/m²; 38 cm wide, 29 cm high) refreshed at 60 Hz and displaying a gray screen of the mean luminance,

positioned 20 cm from the animals' eye. The monitor was γ -corrected by measuring the luminance of the red, green and blue elements with a photometer (Konica Minolta, Chroma meter CS-100A). Neural recordings were aligned to the visual stimulus by the output of a photodiode scanning a small corner of the stimulus monitor shielded from the animal. The coarse location of receptive fields was manually identified and the monitor location adjusted to approximately center them while making the monitor normal to the animal. Receptive field position estimates were subsequently refined by on-line analysis of responses to "sparse-noise," where black or white squares (size 15°; spacing 7.5°, duration 0.2 s) were presented pseudo-randomly at each location of a 9 × 9 grid centered in the monitor, so that the squares spanned 75° × 75° of visual space. Our recordings were made from a variety of elevations in the nasal visual field, or from the lower temporal visual field, and were not distributed sufficiently for us to characterize the relationship between receptive field location and functional properties. We did not correct the display for the distortions in visual angle or changes in illumination that the short viewing distance produces at the edges of the monitor. Stimuli lasted for 2 s with an interstimulus interval of 0.5 s. Each set of stimuli included a blank condition (during which the screen was held at the mean luminance) from which "spontaneous" or maintained firing rates were estimated. Each set of stimuli was presented in pseudo-randomized order for 3–15 repetitions.

In some experiments we presented a drifting sinusoidal grating in a circular patch of varying diameter (2–90°), outside of which the screen was held at the mean luminance. The spatial and temporal frequency of the gratings was determined by initial measurements at each site. We used a spatial frequency near the optimal for the neurons under consideration (usually 0.05 cycles/°; μ 0.09, range 0.04–0.30); temporal frequency was usually 4 Hz (μ 3.5 Hz; 0.7 Hz, n = 2 units; 2 Hz, n = 33; 4 Hz, n = 56; 7.5 Hz, n = 6); Michelson contrast was 0.99 (hereafter normalized to 1.0) unless varied. In additional experiments, we presented a central patch of grating with a surrounding (abutting) annular grating. The central patch was of fixed size, and of the spatial and temporal frequency defined above; the annular grating was of the same spatial frequency, and a temporal frequency 0.5 Hz higher. In one experiment we varied the contrast of the annular grating, and in another experiment, we varied the orientation/direction of the annular grating. Each set of stimuli included trials in which the central patch or an annular grating was presented in isolation. Measurements were drawn from a large set of units, some of which have been reported previously (De Franceschi and Solomon, 2018).

Data analysis

Analysis

Offline analysis was performed in the MATLAB environment (R2019a; The MathWorks). Peristimulus time histograms (PSTHs; bin width 0.016 s) were constructed for each trial, from which we extracted the mean firing rate. Unless stated, we define response as stimulus evoked activity, that is, the change in activity from that measured

during presentation of a blank screen (the spontaneous or maintained firing rate).

Inclusion criteria

We considered neurons visually responsive if their maximal response exceeded the maintained rate by at least 1.5 SD of that rate, and further required that their response exceed two impulses/s in the relevant analysis. We also required the center of a units' receptive field (estimated from responses to the sparse-noise stimulus) to be within 10° of the stimulus center.

Size tuning

To characterize the dependence of response on the size of a grating patch we assumed that both the CRF and a suppressive surround could be described by concentric circular Gaussians (Cavanaugh et al., 2002a). The excitatory CRF (L_e) to a grating of diameter d is proportional to the integrated volume of a Gaussian:

$$L_e(d) = \frac{2}{\sqrt{\pi}} \int_0^d e^{-(x/r_e)^2} dx, \tag{1}$$

where r_e is the width of the Gaussian envelope. A similar expression can be derived for the larger surround Gaussian (L_i). We assumed that the surround has divisive influence on the activity of the CRF (Sceniak et al., 2001; Cavanaugh et al., 2002a), such that response is:

$$R(d) = \frac{K_e L_e(d)}{1 + K_i L_i(d)}, \tag{2}$$

where K_e and K_i are, respectively, the excitatory and the suppressive gains. We found the set of parameters that maximized the log-likelihood (LL) of the model given the responses (El-Shamayleh and Movshon, 2011) using the MATLAB function *fmincon*. We compared the model LL to an upper bound (LL_u ; obtained by fitting the responses to themselves) and a lower bound (LL_l ; obtained by fitting the responses to the average response across all stimuli). The normalized log-likelihood [$LL_n = (LL - LL_l)/(LL_u - LL_l)$] was used to decide whether to include the resulting model parameters in subsequent analyses ($LL_n \geq 0.5$). In addition to the parameters described above we included an additional parameter that allowed for a maintained discharge rate, and included in the set of responses to be modelled the activity during presentation of a blank gray screen. We estimated the preferred size from the model fit as the smallest size reaching 95% of the maximal response.

Suppression index (SI)

To quantify the suppression observed in size-tuning curves we calculated a SI as:

$$SI = 100 \times \frac{R_{opt} - R_{large}}{R_{opt}}, \tag{3}$$

where R_{opt} is the response amplitude at the preferred size and R_{large} is the response amplitude at the largest tested

size; both were extracted from the best predictions of the model above. We used the same expression to quantify suppression in center-surround experiments, substituting R_{opt} with the response to a central patch alone, and R_{large} with the response to the relevant combination of central patch and annular grating.

Adaptation index (AI)

We calculated an AI to characterize the change in response to a stimulus over time:

$$AI = 100 \times \frac{R_{early} - R_{late}}{R_{early}}, \tag{4}$$

where R_{early} and R_{late} are the average evoked activity during the first and last 0.5 s of stimulus presentation, respectively (the stimuli lasted for 2 s).

Orientation/direction tuning

We calculated the direction tuning of stimulus-evoked responses or SI as the amplitude of the vector sum of responses or SI to different directions:

$$gDSI = \frac{\sum R_\theta e^{i\theta}}{\sum R_\theta}, \tag{5}$$

where R_θ is the response to a grating of direction θ . A global index of orientation selectivity is defined in the same way, but after doubling θ . The preferred direction or orientation is the angle of the relevant vector sum. We used the same expression to orientation/direction tuning of surround suppression by substituting R_θ with the SI (SI_θ) measured for an annular grating of direction θ .

Statistics

All statistical comparisons were performed in MATLAB. Correlations are the Pearson's correlation coefficient, r . Statistical tests are Student's paired t tests unless noted.

Results

Most models of receptive fields early in the visual pathway suppose that the signals of different photoreceptors are given appropriate weight (which may be excitatory or inhibitory) and then summed to provide a receptive field that drives spiking output. These models can be used to characterize neurons with center-surround receptive fields as well as those neurons with more complex response properties, such as orientation tuning (Cheong et al., 2013). These models are, however, unable to explain why the response of neurons often depends on the structure of the image beyond the receptive field, or the previous history of stimulation. Explaining these dependencies requires supposing additional spatial and temporal gain controls, which regulate the sensitivity of the receptive field.

The presence of spatial gain controls can be established by measuring the tuning of neurons to the size of a pattern. We therefore varied the diameter of a patch of drifting grating that was centered on the receptive field of

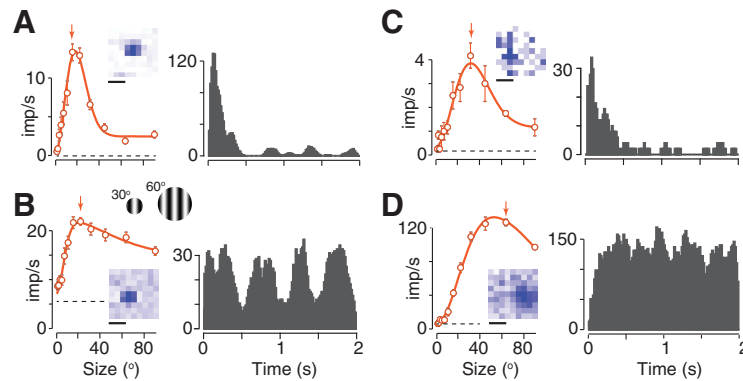


Figure 1. Expression of spatial and temporal gain controls in neurons in SC of awake mouse. **A–D**, Responses of four representative neurons. The left panel in each case shows the average firing rate of the neuron during a 2-s presentation of a circular patch of drifting grating at a spatial frequency near the preferred for the neuron (0.05–0.07 cycles/°), and centered on the receptive field. The right panel in each case shows the PSTH (bin width 0.016 s) during presentation of a patch of grating near the preferred size for that neuron, which is indicated by the arrow in the left panel. Dashed horizontal lines show the maintained rate in absence of patterned visual stimulus. Solid line shows the predictions of the size-tuning model described in Materials and Methods (Eq. 2). Error bars show ± 1 SEM across trials. The insets show a spatial map of responses (white indicates no activity and darker colors indicate stronger responses) to a black square, 15° wide, flashed at each of 81 positions on the monitor. Calibration bars are 26°. The schematic below panel **A** shows the relative size of two patches of grating and how a grating of 0.05 cycles/° would appear in each of them.

the neuron under study (Fig. 1A–D). The response of most neurons was suppressed as the grating extended beyond the receptive field and into the surrounding region, showing the presence of a spatial gain control, or suppressive surround. The presence of temporal gain controls can be established from the time course of response to a visual stimulus. All neurons responded robustly at the onset of a small stimulus. In some neurons, the response was sustained throughout the stimulus duration (Fig. 1B,D), but in others, it was rapidly suppressed (Fig. 1A,C). This adaptation effect shows the presence of a temporal gain control.

Prevalence of spatial and temporal gain controls

We characterized the impact of the spatial gain control as the proportional reduction in response to a large grating (a SI; Eq. 3). Here, values of 0 indicate neurons in which there was no discernible suppression at large sizes, while values of 100 indicate neurons that only responded to small stimuli, and were completely suppressed by larger ones. On average this SI was 76.9% (median 70.4, SD 147.9, $n=93$; Fig. 2A–C), but there was substantial variability across the population of neurons. The absence of suppression in some neurons might arise if their receptive fields are very large, and the gain control was beyond the extent of the stimulus monitor. Our sample included neurons that responded best to the largest grating we could produce, and Figure 2C, filled bars, shows that neurons preferring large gratings (diameter $>30^\circ$) showed little suppression. Most neurons, however, preferred gratings 10–30° in diameter (geometric mean 16.3°, median 15.6°, $n=93$), and in many of these neurons, we saw little suppression although the preferred size was well within the monitor gamut. The measurements above were obtained for patterns of high contrast. To establish the sensitivity of suppression in a sample of neurons we measured the response to a patch of grating of optimal

size, and varied the contrast of an annular grating (data not shown). In these neurons, suppression at 25% annulus contrast was on average 21.6% (SD 15.7, $n=12$), about half that at 100% annulus contrast (38.3, SD 22.0; $p=0.0139$, paired Student's t test). Spatial gain controls can therefore be engaged at low image contrast, and their impact increases with contrast.

To characterize temporal gain control independently from spatial gain control we examined responses to a patch of drifting grating of the preferred size for the neuron under study. We measured the impact of temporal gain controls as the proportional reduction in response from early (the first 0.5 s) to late (the last 0.5 s) time points, producing an AI (Eq. 4) similar to the SI above. On average, later responses were suppressed by 37.4% (median 36.0, SD 33.3, $n=98$; Fig. 2D–F), but as for surround suppression, we saw substantial variability across the population of neurons (Fig. 2F). This variability in AI was not explained by variation in temporal frequency of the grating (2 Hz: μ 33.1%, SD 23.8%, $n=33$; 4 Hz: μ 38.4%, SD 36.1, $n=56$). In a sample of neurons we measured AI for a small patch of grating at low or high contrast (data not shown): the AI at 25% contrast was on average 47.9% (SD 35.0, $n=27$), if anything stronger than at 100% contrast (25.0%, SD 72.1, $n=28$; $p=0.13$, paired Student's t test). Thus, temporal gain controls are also sensitive to low image contrast.

The substantial variability in surround suppression and adaptation's effects raises the question of whether the spatial and temporal gain controls are co-expressed in individual neurons. To establish this, we compared the shape of the size-tuning curves for drifting gratings (provided by the SI) and the time course of response for small patches of drifting grating (provided by the AI). We found strong surround suppression in neurons that showed strong adaptation effects (Fig. 1A,C) and weak surround suppression in neurons that showed weak adaptation

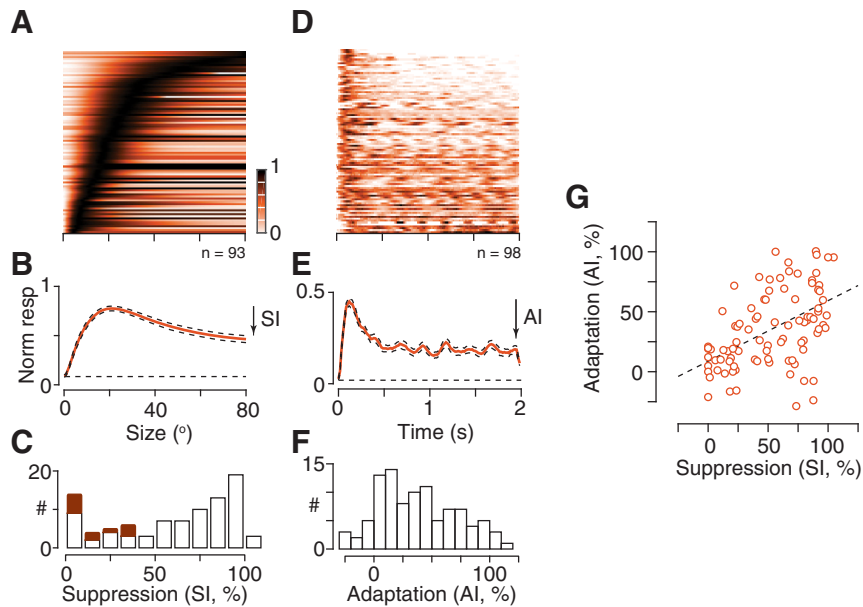


Figure 2. Correlated variability in surround suppression and adaptation effects. **A**, Population size-tuning for patches of drifting gratings. Each row of the image shows the predictions of the size-tuning model for a single neuron (as in Fig. 1), normalized to its maximum response. Only units in which the normalized log-likelihood of the model was at least 0.5 are shown. The units are ordered, from bottom-to-top, by the preferred size. **B**, Mean size-tuning for a drifting grating, obtained by averaging across the rows in **A**. Dashed lines show ± 1 SEM across neurons. Dashed horizontal line shows the maintained rate, normalized to the unit's maximum visual response before averaging. Arrow indicates the definition of the SI, which is the proportional reduction in response from a grating of preferred size to a large grating. **C**, Distribution of the SI across the population of units in **A**. The filled bars show SI for neurons with preferred diameter $>30^\circ$. **D**, Population time course for drifting gratings of preferred size. The units are ordered, from bottom-to-top, by the AI. Color bar as in **A**. **E**, Mean time course for a drifting grating, obtained by averaging across the rows in **D**. Conventions as in **B**. Arrow indicates the definition of the AI, which is the proportional reduction in response from the first 0.5 s to the last 0.5 s. **F**, Distribution of the AI across the population of units in **D**. **G**, Comparison of the SI and AI in individual neurons ($n=93$). Dashed line is the best linear fit to the data.

effects (Fig. 1*B,D*). Consequently, when we compared the index of surround suppression (SI) and the index of adaptation (AI), we found a positive correlation ($r=0.51$, $p<0.00001$, Pearson's correlation coefficient; Fig. 2*G*). Spatial and temporal gain controls therefore appear to be co-expressed in individual neurons.

Many, but not all, neurons in SC are tuned for the orientation or motion direction of a grating. We therefore asked whether this tuning might predict the expression of surround suppression or adaptation effects (data not shown). We found little relationship between adaptation's effects (AI) and global measures of orientation or direction tuning (respectively, $r=0.08$, $r=0.16$; $p=0.47$, $p=0.17$; $n=78$). We found more of a relationship for surround suppression (SI; respectively, $r=0.33$, $r=0.36$; $p=0.0028$, $p=0.0014$). Units with little surround suppression were usually weakly tuned for orientation or direction, while units with strong surround suppression included units with a range of tuning for orientation/direction.

Tuned and untuned contributions to spatial gain controls revealed by adaptation

Inspection of PSTHs for small and large stimuli showed that responses to small stimuli were more transient, that is, adaptation's effects were stronger for small stimuli (Fig. 3*A*). This suggests that spatial and temporal gain

controls interact in shaping neural response. We characterized this interaction by generating size tuning curves for early and late responses. We found less surround suppression at late time points (Fig. 3*B*), and our index of suppression consequently reduced over time (on average from 69.0% to 51.2%, $n=73$, $p<0.00001$, paired Student's *t* test; Fig. 3*C*). The reduced suppression at late time points suggests that surround suppression is also adaptable.

If adaptation changes the sensitivity of surround suppression, it may also change the tuning of surround suppression. Previous work shows that surround suppression in mouse SC can be sensitive to the orientation and/or direction of a pattern (Ahmadlou et al., 2017; Barchini et al., 2018). We confirmed that suppression in SC was usually strongest when the orientation and direction of the annular grating matched that over the receptive field (Fig. 4*A,B*), and in the population average (Fig. 4*E*), suppression was similar for either direction of motion of a parallel annular grating. In other neurons suppression was clearly stronger when the direction of the annular grating also matched that in the central patch, and in others surround suppression was untuned. We therefore asked whether suppression was more tuned in neurons in which spiking response (Fig. 4*A,D*) was also strongly tuned. We used a global index of orientation or direction selectivity (see Materials and Methods) to compare

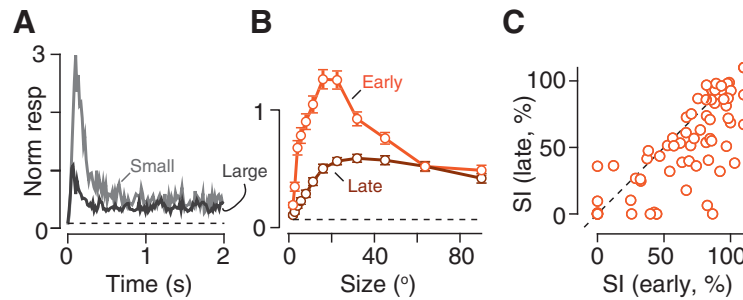


Figure 3. Surround suppression is susceptible to adaptation. **A**, Time course of population response for gratings for small (20° diameter) and large (90°) patches of drifting grating. Responses were normalized to the mean response across all patch sizes (most of which are not shown) before averaging ($n=98$). Dashed horizontal line shows the maintained rate in absence of patterned visual stimulus, normalized in the same way. Error bars are omitted for clarity. **B**, Size-tuning for early (0–0.5 s) and late (1.5–2 s) response, normalized in the same way as **A**. Error bars are ± 1 SEM across neurons that passed criteria for inclusion (early: $n=92$; late: $n=80$). **C**, Comparison of SI for early and late response ($n=73$). Dashed line shows the unity line. Points falling below the line indicate neurons in which suppression was stronger in the early response than in the late response.

the tuning of neuronal responses to a single large grating, with the tuning of suppression elicited by the annular gratings. In both cases, values of 0 indicate no tuning, while values of 1 indicate spiking response or suppression for only one stimulus. There was little correlation ($r = -0.02/0.09$, $p=0.90/0.53$, Pearson's correlation coefficient; Fig. 4C): suppression was often tuned even when spiking response was untuned, and vice versa. Nevertheless, in neurons where the tuning of suppression was strong enough to define a preferred stimulus (tuning index >0.1), the preferred orientation/direction of suppression was generally aligned with the stimulus shown in the central patch (Fig. 4F).

To establish whether the tuning of suppression is changed by adaptation, we measured the tuning of suppression in the first 0.5 s following the onset of the stimulus, and in the last 0.5 s. The population average showed strong suppression at early time points, but this suppression was only weakly tuned for annulus orientation (Fig. 5B). At later time points the overall strength of suppression was reduced and was largely confined to gratings of the same orientation/direction as the central patch, resulting in increased selectivity of suppression (Fig. 5F). To illustrate how tuning changed in individual neurons we compared suppression for annular gratings of the same orientation and motion direction as the central patch, with that for gratings tilted by 45° (average of $\pm 45^\circ$; Fig. 5C,G). Parallel gratings generated stronger suppression at both time points, but their advantage was less pronounced at early (parallel gratings generated μ 21.1% more suppression than tilted gratings, SD 22.3, $n=58$; Fig. 5C,D) than late timepoints (μ 32.6%, SD 31.8, $n=36$; Fig. 5G,H; $p=0.0059$, paired Student's t test, for 35 units that could be characterized at both time points). We conclude that the overall strength of surround suppression reduces over time, and the selectivity of suppression increases.

The pattern of results in Figure 5B,F might be explained if spatial gain controls constitute two mechanisms, one that is narrowly tuned for orientation/direction and less susceptible to adaptation, and one that is more broadly tuned and more susceptible to adaptation. One potential source of suppression is the response of other neurons in SC and we therefore conducted similar analyses of

spiking response to large drifting gratings (Fig. 5A,E). As for suppression, the population spiking response has both tuned and untuned components, and as for suppression the population spiking response reduced substantially at later time points, showing the presence of adaptation effects. This reduction in response was similar for the preferred grating and a grating tilted by 30° ($p=0.0985$, $n=34$). Similar results were obtained if we compared responses to preferred and orthogonal gratings, examined direction tuning curves in a larger dataset including additional units ($n=155$; data not shown), or compared the global orientation and direction selectivity indices. We conclude that adaptation's effects on spiking activity in SC may be sufficient to explain why the overall strength of suppression is reduced at late time points, but additional mechanisms may be required to explain why the tuning of suppression increases at late time points.

Flexible tuning of spatial gain controls

The tuning of spatial gain controls could either be static, or depend on the parameters of the stimulus over the receptive field. In other words, the tuning may be "fixed" or "flexible." In a sample of neurons that were suppressed by annular gratings we therefore repeated the measurements after rotating the orientation/direction of the central patch by 45°. Suppression is relatively broadly tuned, and we therefore expected to see similar tuning curves for suppression across the two measurements. This was the case (Fig. 6A, E). Nevertheless, the most suppressive surround did depend on the orientation/direction of the central patch, at both early (Fig. 6A,B) and late (Fig. 6E,F) time points.

To establish how surround suppression depended on what was shown over the receptive field we focused our analyses on suppression evoked by the pair of annular gratings that matched the orientations/directions of the pair of gratings shown to the receptive field. The orientations of the central gratings over the receptive field are labeled C1 and C2 in Figure 6, and the annulus orientations that matched them are, respectively, S1 and S2. The analyses in Figure 6C,G show that annular gratings were relatively more effective when they matched the central

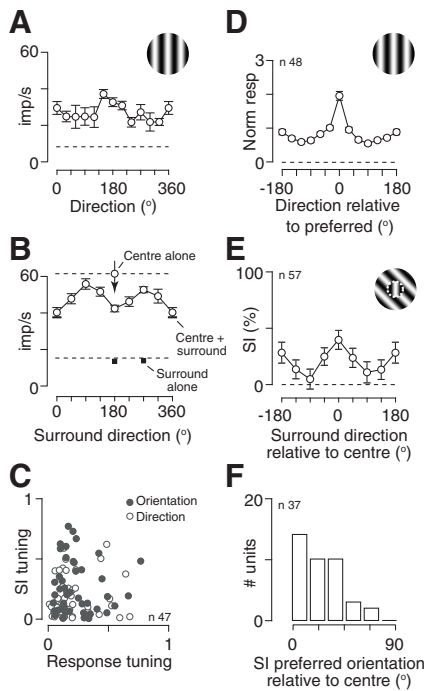


Figure 4. Tuning of surround suppression in SC of awake mouse. **A, B,** Response of an example neuron. **A,** Tuning of spiking activity evoked by a large patch of drifting grating (45° diameter) of varying orientation/direction. Dashed horizontal line shows the maintained rate in absence of patterned visual stimulus. **B,** Tuning of suppression induced by an annular grating of varying orientation/direction. Responses are shown for presentation of a 15° patch of drifting grating (upper dashed line, “center alone”) of direction 180°, the same stimulus when abutted by an annular grating of outer diameter 80° (“center+surround”), and two of the annular gratings presented in absence of the center grating (“surround alone”). The lower dashed horizontal line shows the maintained rate in absence of patterned visual stimulus. A SI can be calculated for each annulus direction as the proportional reduction in response from the “center alone” stimulus to the relevant “center+surround” stimulus. Error bars in **A, B** are ± 1 SEM over trials. **C,** Comparison of tuning for spiking activity (abscissa) and suppression (ordinate). Each unit contributes two points: the open symbols indicate a global measure of direction tuning (Eq. 5) and the filled symbols indicate a similar measure of orientation tuning. **D, E,** Population averages. **D,** Population average spiking activity evoked by a large grating, after aligning each neuron to its preferred direction, subtracting the maintained rate, and then normalizing by the mean response across all stimuli. **E,** Average SI, obtained as in **B,** after aligning each neuron to the direction of the central grating patch. Dashed horizontal line shows an SI of zero. Error bars in **D, E** are ± 1 SEM over neurons. **F,** Distribution of preferred orientation of suppression, relative to the orientation of the center grating, in units in which the preferred orientation could be defined (orientation tuning index > 0.1). A relative orientation of zero indicates neurons in which the most suppressive stimulus was the same orientation as the center; a relative orientation of 90 indicates neurons in which the most suppressive stimulus was orthogonal to the central stimulus. Schematics in panels **A, D, E** are not to scale.

patch. That is, when C1 was the central grating, suppression at S1 was stronger than suppression at S2 (Fig. 6C, G, points lie below the diagonal), and when C2 was the central grating the pattern was reversed (points lie above

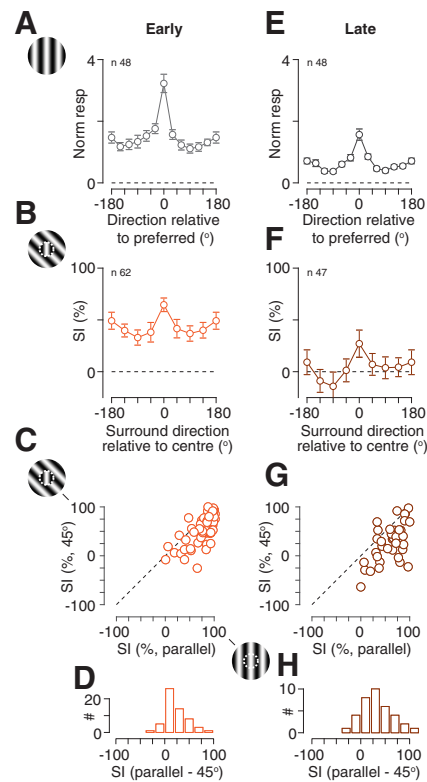


Figure 5. Impact of adaptation on tuning of spiking activity and surround suppression. **A–D,** Responses in early (first 0.5 s) time points. **A,** Population average tuning of spiking activity evoked by a large grating. Conventions as in Figure 4D. **B,** Population average tuning of suppression induced by annular grating. Conventions as in Figure 4E. **C,** Comparison of SI for annular gratings that match the direction of the central grating (“parallel,” abscissa), or are tilted by 45° (ordinate). SI for the latter was averaged across both possible directions of tilt. Dashed lines are the unity line. **D,** Distribution of the difference in suppression for the two annular gratings. Positive indices indicate more suppression by a parallel annulus than a tilted annulus. **E–H,** Same **A–D,** but for late (last 0.5 s) time points. Schematics in panels **A–C** are not to scale.

the diagonal). To compare the suppression that was evoked by S1 and S2 at each of the center orientations we calculated the difference in suppression for the two conditions, that is, for C1 we calculated $SI_{S1} - SI_{S2}$, and for C2 we also calculated $SI_{S1} - SI_{S2}$. This subtraction collapsed the data along the diagonal in Figure 6C,G while preserving sign, and produced the distributions in Figure 6D,H.

The advantage of matched annular gratings appeared to increase with time: suppression indices lie further away from the diagonal at later time points (Fig. 6G) than they do at early time points (Fig. 6C). Similarly, the distributions in Figure 6H lie further from 0 than do the distributions in Figure 6D. To provide a statistical comparison across early and late time points, we computed an additional index, $[MI = (SI_{C1,S1} - SI_{C1,S2}) - (SI_{C2,S1} - SI_{C2,S2})]$ for each unit at each time point. If suppression was fixed, and thus the same for any particular annulus orientation, regardless of center orientation, then this MI should be 0, but it was

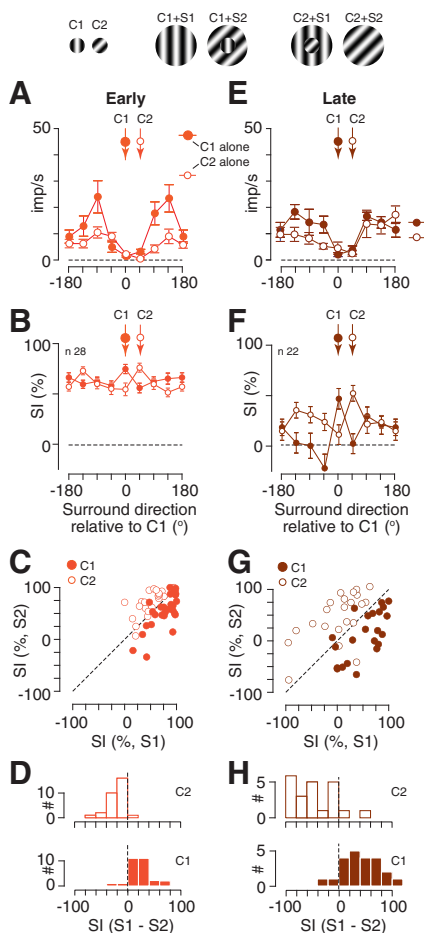


Figure 6. Adaptation's effects magnify flexible surround suppression. **A–D**, Responses in early (first 0.5 s) time points. **A**, Spiking activity of an example neuron during presentation of a central stimulus either presented alone (C1, C2), or abutting an annulus of varying direction. Two measurements were made, first with a central grating near the preferred direction of spiking activity (C1) and then with a central grating tilted by 45° (C2). Error bars are ± 1 SEM over trials. **B**, Population average tuning of suppression for each of two central gratings (C1, C2). Conventions as in Figure 4E. **C**, Comparison of suppression induced by pairs of stimuli. The abscissa shows the suppression induced by an annular grating (S1) that matched the direction of the central grating C1. The ordinate shows the suppression induced by an annular grating (S2) that matched the central grating C2. Points below the unity line (dashed line) indicate stronger suppression for S1 than S2. Filled circles show measurements obtained with C1: these generally lie below the unity line, indicating that when C1 is used, S1 is more effective than S2. Open circles show measurements obtained for C2: measurements are generally above the unity line, indicating that S2 is more effective than S1. This is the pattern of results expected if suppression is stronger when the stimuli over the center and surround are matched. **D**, Distribution of the difference in suppression for each of the center gratings, C1 (lower) and C2 (upper). Positive indices indicate more suppression by S1 than S2. **E–H**, Same as **A–D** but for late (last 0.5 s) time points. Example neuron in **E** is the same as that in **A**. Schematics above **A**, **E** are not to scale.

not (early: μ 40.4, SD 33.1, $n=28$; late: μ 85.4, SD 60.1, $n=22$). Comparison of the indices at early and late time points, for units that responded in both, showed that the index increased at later time points ($p=0.000459$, $n=22$; paired Student's t test). We conclude that the tuning of suppression in SC can be flexible, and that this flexibility is most apparent at later time points, when the untuned gain control is less effective.

Discussion

Functional impact of temporal gain controls

Adaptation's effects allow neurons to adjust their activity to the recent stimulus history. The reduction in response to a stimulus that is unchanging might be used by neurons to better signal changes over time. We have shown that many neurons in the mouse SC show adaptation effects: responses are characterized by a large initial response that is quickly suppressed. This suppression cannot be explained by retinal light adaptation, because we presented drifting gratings, where the spatial pattern is constantly modulated.

The timescales of adaptation effects that we have characterized are on the order of 10–100s of milliseconds, shorter than most earlier characterizations of adaptation effects in SC, which were primarily conducted in anaesthetized animals (e.g., rabbit: Horn and Hill, 1966; monkey: Cynader and Berman, 1972; mouse: Dräger and Hubel, 1975; pigeon: Woods and Frost, 1977). That work emphasized a large and long-lasting suppression of response (often called habituation). The habituation was strongest in the intermediate and deeper layers of the SC, but it has also been reported in the superficial layers (rabbit: Oyster and Takahashi, 1975; cat: Binns and Salt, 1995). In anaesthetized rat, more rapid adaptation effects were seen in superficial neurons for flashes of bright spots on a dark background (Bytautiene and Baranauskas, 2018), but those effects may have included a contribution of light adaptation. Our stimuli were interleaved, and were preceded by other sets of stimuli, so it is difficult to establish the effect of long-term habituation from these measurements. Nevertheless, we did not see a clear impact of position in the stimulus sequence on response amplitude, even when we only considered units with high adaptation indices (data not shown). Recordings in superficial layers of awake monkey also show lack of long-term adaptation effects (Goldberg and Wurtz, 1972), and more substantial short-term adaptation effects (Mayo and Sommer, 2008; Boehnke et al., 2011).

Previous measurements of adaptation's effect in SC have often involved repeated presentation of a brief stimulus (Boehnke et al., 2011), whereas we measured response to a single, longer, continuous stimulus. While the two types of stimuli are likely to engage the same mechanisms, that does not mean they will have the same effect (Solomon and Kohn, 2014). The transients associated with repeated flashes may be more effective at driving the adaptive mechanism(s) and repeated presentations may therefore induce greater changes in activity. Alternatively, the periods of rest between the presentations may allow adaptive

mechanisms to recover, and repeated presentations may therefore have less effect. Onset transients appear to be increasingly important for information processing as one ascends through the visual hierarchy (Tovée et al., 1993; Müller et al., 2001), so differences in adaptive responses to repeated and continuous presentations may be more pronounced in later visual processing. SC integrates early and later visual inputs, so comparison of adaptive responses to flashed and continuous presentation may be of interest.

Adaptation effects are prominent in retinal ganglion cell response, and likely first emerge in the bipolar cell input to ganglion cells (salamander: Chander and Chichilnisky, 2001; salamander/rabbit: Baccus and Meister, 2002; monkey: Solomon et al., 2004; guinea pig: Zaghoul et al., 2005; mouse: Marco et al., 2013). It is therefore probable that some of the adaptation effects that we see in SCs are inherited from the retinal input, but we are not aware of reports of retinal neurons that show the complete suppression of response that we often encountered in SCs. Additional mechanisms in SCs, potentially mediated by GABA_B receptors and metabotropic glutamate receptors, have been implicated in presynaptic and postsynaptic adaptation effects in SCs (cat: Binns and Salt, 1995; rat: Cirone and Salt, 2001), and these are likely to enhance or supersede adaptation effects inherited from retinal input. In addition, the sustained response was slightly reduced at large stimulus sizes (compare with Fig. 3A), while the initial transient was strongly reduced. Size-dependence of the sustained response has also been observed in SC of monkey (Chen and Hafed, 2018), although direct comparison is difficult because that work explored shorter time-windows and stimuli confined to the receptive field.

Functional impact of spatial gain controls

Suppressive surrounds have been described in the SC of many species (cat: Sterling and Wickelgren, 1969; monkey: Cynader and Berman, 1972; Wurtz et al., 1980; rat: Girman and Lund, 2007; zebrafish: Del Bene et al., 2010; barn owl: Mysore et al., 2010; Zahar et al., 2012, 2018), including mouse (Wang et al., 2010; Gale and Murphy, 2014; Ahmadlou et al., 2017; Barchini et al., 2018). We show that in awake mouse surround suppression consists of at least two components, one that is weakly tuned and adaptable, and another that is more tuned and less susceptible to adaptation's effects. The tuned gain controls appear to have flexible selectivity, such that the most suppressive surrounding stimulus is that which matches the stimulus over the receptive field.

Most types of mouse retinal ganglion cell send axons to the SCs (Ellis et al., 2016), and several of these are known to show surround suppression. One is the ON-OFF W3 cell (Zhang et al., 2012), thought to be a homolog of the "net convexity detector" cells in the frog retina (Lettvin et al., 1959) and the local edge detector (LED) cells first described in rabbit (Levick, 1967). But size sensitive responses are also found in "high-definition" (HD; Jacoby and Schwartz, 2017) as well as the direction-selective J and BD retinal ganglion cell classes, which also project to SCs (Kim et al., 2010). Thus, some of the surround suppression that we observe in SCs may be inherited from

the retinal input. Yet while adaptation effects can reduce the amount of inhibition onto retinal ganglion cells (salamander/rabbit: Baccus and Meister, 2002; mouse: Wark et al., 2009; Marco et al., 2013; salamander: Kastner et al., 2019), we are not aware of reports of adaptation effects on suppression in retina at the time scale of the rapid adaptation that we see in SCs. This suggests that lateral interactions within SCs are a strong contributor to the surround suppression that we see, and the simplest conclusion is that adaptation reduces surround suppression in SCs because adaptation reduces spiking activity in SCs.

Networks in the superficial layers of mouse SC include inhibitory lateral interactions that suppress the activity of simultaneously activated neurons (Phongphanphane et al., 2014). Local inhibition from "horizontal cells," which respond to large stimuli (Gale and Murphy, 2014), may be particularly important in providing surround suppression (Gale and Murphy, 2016), while "narrow field" and "wide field" cells appear particularly susceptible to suppression (Gale and Murphy, 2014). Similar mechanisms for constructing size tuning have been described in the zebrafish optic tectum (Del Bene et al., 2010). In addition, the SC receives substantial input from visual cortex (May, 2006), although the role(s) of cortico-collicular input remain unclear, these projections modulate gain of SC neurons but their absence seems to have little effect on tuning properties (Wang et al., 2010; Zhao et al., 2014) or surround suppression (Ahmadlou et al., 2017), at least in mouse. Indeed, surround suppression in the SC may precede that in primary visual cortex (V1; monkey: White et al., 2017) and inactivation of SC can interfere with surround suppression in V1 of mouse (Ahmadlou et al., 2018).

Units that were not selective for pattern orientation/direction were also less likely to show strong surround suppression. This result may reflect a straightforward correlation in the two functional properties, or surround suppression may be important for constructing selectivity for orientation or direction. Regardless, controlling for the size of stimuli is likely to be important in characterizing, and therefore understanding, the mechanisms of orientation and direction tuning in SC.

We found that tuned surround suppression was less susceptible to adaptation than untuned suppression, with the consequence that suppression was more sharply tuned and more flexible in later activity. Our finding that at least some of the suppression in SCs is flexible is in accord with recent calcium imaging from SCs of anesthetized mouse (Barchini et al., 2018). That work showed suppression by surrounding gratings of the same motion direction as a central patch, and facilitation by surrounds of the opposite direction, particularly in excitatory cells. The dynamics of calcium signaling make comparison of response time course difficult, but the initial spiking response, where we find weakly tuned suppression, may have contributed less to the calcium signal than the subsequent response, where we find more tuning of suppression and some facilitation. Our finding that tilted surrounds could even become facilitatory in the late phase of responses raises the possibility that the tuning of late suppression may in fact reflect tuned facilitation. Flexible

suppression selectivity may therefore reflect input from neurons with large receptive fields that are sensitive to image continuity (if they provide tuned suppression) or sensitive to image discontinuity (if they provide tuned facilitation). These flexible mechanisms may arise in SCs or in its inputs. If they arise in SCs, then one candidate may be the horizontal cells. Regardless, mouse SCs is likely to be a useful model for understanding the mechanisms that enable flexible suppression of neural responses by spatial context (Coen-Cagli et al., 2015).

The functional properties of surround suppression in SCs are remarkably similar to that described for V1 in many mammals. First, surround suppression in V1 is often orientation-selective and direction-selective (mouse: Self et al., 2014; cat: Nelson and Frost, 1978; DeAngelis et al., 1994; Ozeki et al., 2004; monkey: Sillito et al., 1995; Levitt and Lund, 1997; Cavanaugh et al., 2002b; Webb et al., 2005; Henry et al., 2013), and that tuning selectivity can be flexible (Sillito et al., 1995; Cavanaugh et al., 2002b). Second, in V1 of mouse, monkey, and human, this tuned suppression is complemented by an untuned suppression (mouse: Self et al., 2014; monkey: Webb et al., 2005; Henry et al., 2013; human: Schallmo et al., 2019), some of which may be inherited from earlier processing (cat/monkey: Sillito et al., 1993; cat: Ozeki et al., 2004; Bonin et al., 2005; Naito et al., 2007; monkey: Solomon et al., 2002; Camp et al., 2009). Third, some components of surround suppression in V1 of monkey and human are susceptible to adaptation (Cavanaugh et al., 2002a; Wissig and Kohn, 2012; Patterson et al., 2013; Schallmo and Murray, 2016), although in monkey V1, the tuned components of suppression may be more sensitive to adaptation than the untuned components (Webb et al., 2005).

Summary

We have shown the presence of spatial and temporal gain controls in SCs of awake mouse and how they are distributed across neurons. Our results are consistent with the idea that these gain controls provide a predictive signal against which activation of the CRF is compared, thereby suppressing the response to predictable stimuli and highlighting unexpected ones. Our results can be accommodated by a layering of gain controls as illustrated in Figure 7. Figure 7A shows the standard model of early visual processing (Carandini and Heeger, 2011; Solomon and Kohn, 2014). The output of the CRF, which filters the visual image, is subject to a spatial gain control, or suppressive surround, before driving spiking activity. The suppressive surround is constructed from nearby neurons with similar characteristics. Adaptation's effects can be thought of as changing the output function of the neuron, as shown by the red-line in Figure 7B. This accounts for the results in Figure 5, because similar neurons contribute to the surround, and the surround is therefore relatively broadly tuned for orientation/direction and susceptible to

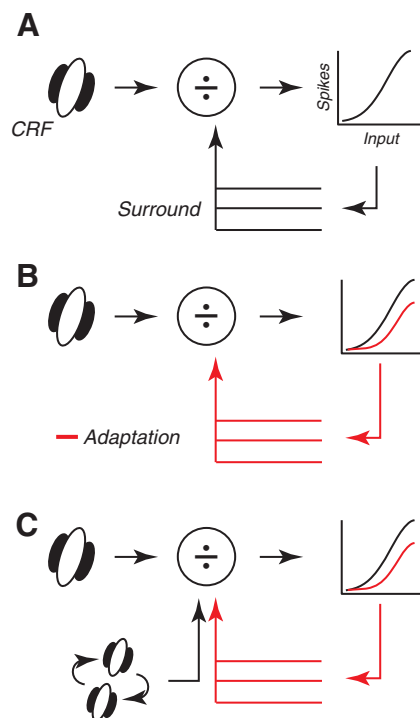


Figure 7. Descriptive model for interaction of spatial and temporal gain controls in SCs. **A**, Standard model of receptive fields early in the visual pathway. The CRF filters the visual image, and its output is subject to a spatial gain control (surround) before driving spiking output. The surround is comprised of units with receptive fields similar to that of the CRF. **B**, Adaptation's effects reduce the response of the neuron under study, and the responses of neurons that contribute to the spatial gain control. **C**, Addition of a second, less adaptable, component to the spatial gain control allows for preservation of suppression when the features of the image over the CRF matches that over the surround.

adaptation's effects. To account for the advantage of surrounds that match the center stimulus (Fig. 6), and the apparent resilience of this suppression to adaptation's effects, a second mechanism seems to be required (Fig. 7C). This is sensitive to the relationship between features over the CRF and surround and is less adaptable.

We also found that the strength of adaptation's effects and strength of surround suppression were correlated among neurons. Our results therefore show that neurons characterized by a transient, adapting response are more likely to also be affected by spatial context, and may therefore signal the presence of unexpected objects in either the spatial and the temporal domain. This suggests the presence of a subpopulation of "novelty" or "saliency" neurons within the SC that are sensitive to unexpected events in the visual diet. Whether this functional subgroup has an anatomic correlate would be of interest. In monkey, the amplitude of the initial transient response in anatomically deeper visual-motor SC neurons, which receive direct input from the superficial purely visual neurons studied here, is known to be particularly important in the nature and latency of orienting behaviors such as saccades (Boehnke and Munoz, 2008; Chen and Hafed, 2017).

References

- Adesnik H, Bruns W, Taniguchi H, Huang ZJ, Scanziani M (2012) A neural circuit for spatial summation in visual cortex. *Nature* 490:226–231.
- Ahmadlou M, Tafreshiha A, Heimel JA (2017) Visual cortex limits pop-out in the superior colliculus of awake mice. *Cereb Cortex* 27:5772–5783.
- Ahmadlou M, Zweifel LS, Heimel JA (2018) Functional modulation of primary visual cortex by the superior colliculus in the mouse. *Nat Commun* 9:3895.
- Allman J, Miezin F, McGuinness E (1985) Stimulus specific responses from beyond the classical receptive field: neurophysiological mechanisms for local-global comparisons in visual neurons. *Annu Rev Neurosci* 8:407–430.
- Baccus SA, Meister M (2002) Fast and slow contrast adaptation in retinal circuitry. *Neuron* 36:909–919.
- Barchini J, Shi X, Chen H, Cang J (2018) Bidirectional encoding of motion contrast in the mouse superior colliculus. *Elife* 7:e35261.
- Barlow H (2001) The exploitation of regularities in the environment by the brain. *Behav Brain Sci* 24:602–607; discussion 652–671.
- Basso MA, May PJ (2017) Circuits for action and cognition: a view from the superior colliculus. *Annu Rev Vis Sci* 3:197–226.
- Binns KE, Salt TE (1995) Excitatory amino acid receptors modulate habituation of the response to visual stimulation in the cat superior colliculus. *Vis Neurosci* 12:563–571.
- Boehnke SE, Munoz DP (2008) On the importance of the transient visual response in the superior colliculus. *Curr Opin Neurobiol* 18:544–551.
- Boehnke SE, Berg DJ, Marino RA, Baldi PF, Itti L, Munoz DP (2011) Visual adaptation and novelty responses in the superior colliculus. *Eur J Neurosci* 34:766–779.
- Bonds AB (1989) Role of inhibition in the specification of orientation selectivity of cells in the cat striate cortex. *Vis Neurosci* 2:41–55.
- Bonin V, Mante V, Carandini M (2005) The suppressive field of neurons in lateral geniculate nucleus. *J Neurosci* 25:10844–10856.
- Bytautiene J, Baranauskas G (2018) Experimentally derived model shows that adaptation acts as a powerful spatiotemporal filter of visual responses in the rat collicular neurons. *Sci Rep* 8:8942.
- Camp AJ, Tailby C, Solomon SG (2009) Adaptable mechanisms that regulate the contrast response of neurons in the primate lateral geniculate nucleus. *J Neurosci* 29:5009–5021.
- Carandini M, Ferster D (1997) A tonic hyperpolarization underlying contrast adaptation in cat visual cortex. *Science* 276:949–952.
- Carandini M, Heeger DJ (2011) Normalization as a canonical neural computation. *Nat Rev Neurosci* 13:51–62.
- Cavanaugh JR, Bair W, Movshon JA (2002a) Nature and interaction of signals from the receptive field center and surround in macaque V1 neurons. *J Neurophysiol* 88:2530–2546.
- Cavanaugh JR, Bair W, Movshon JA (2002b) Selectivity and spatial distribution of signals from the receptive field surround in macaque V1 neurons. *J Neurophysiol* 88:2547–2556.
- Chander D, Chichilnisky EJ (2001) Adaptation to temporal contrast in primate and salamander retina. *J Neurosci* 21:9904–9916.
- Chen CY, Hafed ZM (2017) A neural locus for spatial-frequency specific saccadic suppression in visual-motor neurons of the primate superior colliculus. *J Neurophysiol* 117:1657–1673.
- Chen CY, Hafed ZM (2018) Orientation and contrast tuning properties and temporal flicker fusion characteristics of primate superior colliculus neurons. *Front Neural Circuits* 12:58.
- Cheong SK, Tailby C, Solomon SG, Martin PR (2013) Cortical-like receptive fields in the lateral geniculate nucleus of marmoset monkeys. *J Neurosci* 33:6864–6876.
- Cirone J, Salt TE (2001) Group II and III metabotropic glutamate receptors contribute to different aspects of visual response processing in the rat superior colliculus. *J Physiol* 534:169–178.
- Coen-Cagli R, Kohn A, Schwartz O (2015) Flexible gating of contextual influences in natural vision. *Nat Neurosci* 18:1648–1655.
- Comoli E, Das Neves Favaro P, Vautrelle N, Leriche M, Overton PG, Redgrave P (2012) Segregated anatomical input to sub-regions of the rodent superior colliculus associated with approach and defense. *Front Neuroanat* 6:9.
- Cynader M, Berman N (1972) Receptive-field organization of monkey superior colliculus. *J Neurophysiol* 35:187–201.
- Davidson RM, Bender DB (1991) Selectivity for relative motion in the monkey superior colliculus. *J Neurophysiol* 65:1115–1133.
- Dean P, Redgrave P, Westby GW (1989) Event or emergency? Two response systems in the mammalian superior colliculus. *Trends Neurosci* 12:137–147.
- DeAngelis GC, Freeman RD, Ohzawa I (1994) Length and width tuning of neurons in the cat's primary visual cortex. *J Neurophysiol* 71:347–374.
- De Franceschi G, Solomon SG (2018) Visual response properties of neurons in the superficial layers of the superior colliculus of awake mouse. *J Physiol* 596:6307–6332.
- Del Bene F, Wyart C, Robles E, Tran A, Looger L, Scott EK, Isacoff EY, Baier H (2010) Filtering of visual information in the tectum by an identified neural circuit. *Science* 330:669–673.
- Dräger UC, Hubel DH (1975) Responses to visual stimulation and relationship between visual, auditory, and somatosensory inputs in mouse superior colliculus. *J Neurophysiol* 38:690–713.
- Dutta A, Gutfreund Y (2014) Saliency mapping in the optic tectum and its relationship to habituation. *Front Integr Neurosci* 8:1.
- El-Shamayleh Y, Movshon JA (2011) Neuronal responses to texture-defined form in macaque visual area V2. *J Neurosci* 31:8543–8555.
- Ellis EM, Gauvain G, Sivyer B, Murphy GJ (2016) Shared and distinct retinal input to the mouse superior colliculus and dorsal lateral geniculate nucleus. *J Neurophysiol* 116:602–610.
- Fisher TG, Aliitto HJ, Usrey WM (2017) Retinal and nonretinal contributions to extraclassical surround suppression in the lateral geniculate nucleus. *J Neurosci* 37:226–235.
- Gale SD, Murphy GJ (2014) Distinct representation and distribution of visual information by specific cell types in mouse superficial superior colliculus. *J Neurosci* 34:13458–13471.
- Gale SD, Murphy GJ (2016) Active dendritic properties and local inhibitory input enable selectivity for object motion in mouse superior colliculus neurons. *J Neurosci* 36:9111–9123.
- Girman SV, Lund RD (2007) Most superficial sublamina of rat superior colliculus: neuronal response properties and correlates with perceptual figure-ground segregation. *J Neurophysiol* 98:161–177.
- Goldberg ME, Wurtz RH (1972) Activity of superior colliculus in behaving monkey. I. Visual receptive fields of single neurons. *J Neurophysiol* 35:542–559.
- Hartline HK (1940) The receptive fields of optic nerve fibers. *Am J Physiol* 130:690–699.
- Henry CA, Joshi S, Xing D, Shapley RM, Hawken MJ (2013) Functional characterization of the extraclassical receptive field in macaque V1: contrast, orientation, and temporal dynamics. *J Neurosci* 33:6230–6242.
- Horn G, Hill RM (1966) Responsiveness to sensory stimulation of units in the superior colliculus and subjacent tectotegmental regions of the rabbit. *Exp Neurol* 14:199–223.
- Hoy JL, Bishop HI, Niell CM (2019) Defined cell types in superior colliculus make distinct contributions to prey capture behavior in the mouse. *Curr Biol* 29:4130–4138.e5.
- Jacoby J, Schwartz GW (2017) Three small-receptive-field ganglion cells in the mouse retina are distinctly tuned to size, speed, and object motion. *J Neurosci* 37:610–625.
- Jones HE, Andolina IM, Oakley NM, Murphy PC, Sillito AM (2000) Spatial summation in lateral geniculate nucleus and visual cortex. *Exp Brain Res* 135:279–284.
- Kastner DB, Ozuyal Y, Panagiotakos G, Baccus SA (2019) Adaptation of inhibition mediates retinal sensitization. *Curr Biol* 29:2640–2651.e4.
- Kim IJ, Zhang Y, Meister M, Sanes JR (2010) Laminar restriction of retinal ganglion cell dendrites and axons: subtype-specific developmental patterns revealed with transgenic markers. *J Neurosci* 30:1452–1462.

- Kuffler SW (1953) Discharge patterns and functional organization of mammalian retina. *J Neurophysiol* 16:37–68.
- Lettvin JY, Maturana HR, McCulloch WS, Pitts WH (1959) What the frog's eye tells the frog's brain. *Proc IRE* 47:1940–1951.
- Levick WR (1967) Receptive fields and trigger features of ganglion cells in the visual streak of the rabbits retina. *J Physiol* 188:285–307.
- Levitt JB, Lund JS (1997) Contrast dependence of contextual effects in primate visual cortex. *Nature* 387:73–76.
- Marco SD, Protti DA, Solomon SG (2013) Excitatory and inhibitory contributions to receptive fields of alpha-like retinal ganglion cells in mouse. *J Neurophysiol* 110:1426–1440.
- May PJ (2006) The mammalian superior colliculus: laminar structure and connections. *Prog Brain Res* 151:321–378.
- Mayo JP, Sommer MA (2008) Neuronal adaptation caused by sequential visual stimulation in the frontal eye field. *J Neurophysiol* 100:1923–1935.
- Movshon JA, Lennie P (1979) Pattern-selective adaptation in visual cortical neurones. *Nature* 278:850–852.
- Müller JR, Metha AB, Krauskopf J, Lennie P (2001) Information conveyed by onset transients in responses of striate cortical neurons. *J Neurosci* 21:6978–6990.
- Mysore SP, Asadollahi A, Knudsen EI (2010) Global inhibition and stimulus competition in the owl optic tectum. *J Neurosci* 30:1727–1738.
- Naito T, Sadakane O, Okamoto M, Sato H (2007) Orientation tuning of surround suppression in lateral geniculate nucleus and primary visual cortex of cat. *Neuroscience* 149:962–975.
- Nelson JI, Frost BJ (1978) Orientation-selective inhibition from beyond the classic visual receptive field. *Brain Res* 139:359–365.
- Oyster CW, Takahashi ES (1975) Responses of rabbit superior colliculus neurons to repeated visual stimuli. *J Neurophysiol* 38:301–312.
- Ozeki H, Sadakane O, Akasaki T, Naito T, Shimegi S, Sato H (2004) Relationship between excitation and inhibition underlying size tuning and contextual response modulation in the cat primary visual cortex. *J Neurosci* 24:1428–1438.
- Patterson CA, Wissig SC, Kohn A (2013) Distinct effects of brief and prolonged adaptation on orientation tuning in primary visual cortex. *J Neurosci* 33:532–543.
- Phongphananee P, Marino RA, Kaneda K, Yanagawa Y, Munoz DP, Isa T (2014) Distinct local circuit properties of the superficial and intermediate layers of the rodent superior colliculus. *Eur J Neurosci* 40:2329–2343.
- Rossant C, Kadir SN, Goodman DFM, Schulman J, Hunter MLD, Saleem AB, Grosmark A, Belluscio M, Denfield GH, Ecker AS, Tolias AS, Solomon S, Buzsaki G, Carandini M, Harris KD (2016) Spike sorting for large, dense electrode arrays. *Nat Neurosci* 19:634–641.
- Sceniak MP, Hawken MJ, Shapley R (2001) Visual spatial characterization of macaque V1 neurons. *J Neurophysiol* 85:1873–1887.
- Schallmo MP, Murray SO (2016) Identifying separate components of surround suppression. *J Vis* 16:2.
- Schallmo MP, Kale AM, Murray SO (2019) The time course of different surround suppression mechanisms. *J Vis* 19:12.
- Self MW, Lorteije JA, Vangeneugden J, van Beest EH, Grigore ME, Levelt CN, Heimel JA, Roelfsema PR (2014) Orientation-tuned surround suppression in mouse visual cortex. *J Neurosci* 34:9290–9304.
- Shapley RM, Victor JD (1978) The effect of contrast on the transfer properties of cat retinal ganglion cells. *J Physiol* 285:275–298.
- Shi X, Barchini J, Ledesma HA, Koren D, Jin Y, Liu X, Wei W, Cang J (2017) Retinal origin of direction selectivity in the superior colliculus. *Nat Neurosci* 20:550–558.
- Sillito AM, Cudeiro J, Murphy PC (1993) Orientation sensitive elements in the corticofugal influence on centre-surround interactions in the dorsal lateral geniculate nucleus. *Exp Brain Res* 93:6–16.
- Sillito AM, Grieve KL, Jones HE, Cudeiro J, Davis J (1995) Visual cortical mechanisms detecting focal orientation discontinuities. *Nature* 378:492–496.
- Smirnakis SM, Berry MJ, Warland DK, Bialek W, Meister M (1997) Adaptation of retinal processing to image contrast and spatial scale. *Nature* 386:69–73.
- Solomon SG, Kohn A (2014) Moving sensory adaptation beyond suppressive effects in single neurons. *Curr Biol* 24:R1012–R1022.
- Solomon SG, White AJ, Martin PR (2002) Extraclassical receptive field properties of parvocellular, magnocellular, and koniocellular cells in the primate lateral geniculate nucleus. *J Neurosci* 22:338–349.
- Solomon SG, Peirce JW, Dhruv NT, Lennie P (2004) Profound contrast adaptation early in the visual pathway. *Neuron* 42:155–162.
- Solomon SG, Lee BB, Sun H (2006) Suppressing surrounds and contrast gain in magnocellular-pathway retinal ganglion cells of macaque. *J Neurosci* 26:8715–8726.
- Srinivasan MV, Laughlin SB, Dubs A (1982) Predictive coding: a fresh view of inhibition in the retina. *Proc R Soc Lond B Biol Sci* 216:427–459.
- Sterling P, Wickelgren BG (1969) Visual receptive fields in the superior colliculus of the cat. *J Neurophysiol* 32:1–15.
- Tovée MJ, Rolls ET, Treves A, Bellis RP (1993) Information encoding and the responses of single neurons in the primate temporal visual cortex. *J Neurophysiol* 70:640–654.
- Vaiceilunaite A, Erisken S, Franzen F, Katzner S, Busse L (2013) Spatial integration in mouse primary visual cortex. *J Neurophysiol* 110:964–972.
- Wang L, Sarnaik R, Rangarajan K, Liu X, Cang J (2010) Visual receptive field properties of neurons in the superficial superior colliculus of the mouse. *J Neurosci* 30:16573–16584.
- Wark B, Fairhall A, Rieke F (2009) Timescales of inference in visual adaptation. *Neuron* 61:750–761.
- Webb BS, Dhruv NT, Solomon SG, Tailby C, Lennie P (2005) Early and late mechanisms of surround suppression in striate cortex of macaque. *J Neurosci* 25:11666–11675.
- Webster MA (2015) Visual adaptation. *Annu Rev Vis Sci* 1:547–567.
- White BJ, Kan JY, Levy R, Itti L, Munoz DP (2017) Superior colliculus encodes visual saliency before the primary visual cortex. *Proc Natl Acad Sci USA* 114:9451–9456.
- Wissig SC, Kohn A (2012) The influence of surround suppression on adaptation effects in primary visual cortex. *J Neurophysiol* 107:3370–3384.
- Woods EJ, Frost BJ (1977) Adaptation and habituation characteristics of tectal neurons in the pigeon. *Exp Brain Res* 27:347–354.
- Wurtz RH, Richmond BJ, Judge SJ (1980) Vision during saccadic eye movements. III. Visual interactions in monkey superior colliculus. *J Neurophysiol* 43:1168–1181.
- Zaghloul KA, Boahen K, Demb JB (2005) Contrast adaptation in sub-threshold and spiking responses of mammalian Y-type retinal ganglion cells. *J Neurosci* 25:860–868.
- Zahar Y, Wagner H, Gutfreund Y (2012) Responses of tectal neurons to contrasting stimuli: an electrophysiological study in the barn owl. *PLoS One* 7:e39559.
- Zahar Y, Lev-Ari T, Wagner H, Gutfreund Y (2018) Behavioral evidence and neural correlates of perceptual grouping by motion in the barn owl. *J Neurosci* 38:6653–6664.
- Zhang Y, Kim IJ, Sanes JR, Meister M (2012) The most numerous ganglion cell type of the mouse retina is a selective feature detector. *Proc Natl Acad Sci USA* 109:E2391–E2398.
- Zhao X, Liu M, Cang J (2014) Visual cortex modulates the magnitude but not the selectivity of looming-evoked responses in the superior colliculus of awake mice. *Neuron* 84:202–213.